Simulations of ICF Hohlraum and Radiation Hydrodynamics in a Plastic Foil

N. K. Gupta, T. C. Kaushik and B. K. Godwal
High Pressure Physics Division, Bhabha Atomic Research Centre,
Trombay, Mumbai –400 085, India.

e-mail: nkgupta@apsara.barc.ernet.in

Abstract. In this paper we study the effects of various parameters on the estimation of radiation temperature inside indirect drive ICF hohlraum and compare results with the published work. A multi group, 1-D, cylindrical geometry, radiation hydrodynamic code is used for this study. The radiation temperature inside a cylindrical hohlraum is seen to be strongly dependent on the number of frequency groups used. It is also seen that erroneous results can be obtained if the space mesh in the hohlraum wall is not fine enough. The spectrum of the radiation is also seen to be different from Planck, especially in the high-energy range. Hydrodynamics of a CHBr foil driven by the hohlraum radiation brings about the need of a proper equation of state model. A three term equation of state is used for these studies and data for CHBr is generated by scaling density, atomic number and weight of the high-density polysterene (CH)n to that of CHBr.

1. Introduction

Most of the contemporary inertial confinement fusion (ICF) experiments are based on the concept of indirect-drive, although some of the recent smoothening devices like random phase plate (RPP), spectral dispersion (SSD), induced spatial incoherence (IST) have kept interest alive in direct drive targets. Indirect drive fusion schemes first convert the incident laser or ion beams to soft X rays and then use these radiation to drive the target. These devices have a distinctive advantage of uniform radiation inside. This uniformity of the radiation inside the hohlraum is of great significance for the success of ICF experiments. The present experiments on equation of state measurements are essentially using the hohlraum as a source of soft X-rays to drive the shock wave in the material. The pressures as high as 750 Mbars are reported to have been achieved [1]. Even the alternate driver schemes such as capacitor bank driven imploding plasma liners finally aim to convert the energy into hohlraums with good success [2] already demonstrated. To minimize the energy loss in converting primary energy from laser or ion beam to X-rays, high absorption and reemission from hohlraum walls are required. For this the high Z material like gold are widely used for the hohlraum walls although, recently, composite materials are also proposed for this purpose [3]. To numerically simulate an indirect drive ICF experiment, the two basic requirements are the radiation hydrodynamics and the computations of the frequency dependent radiation opacities. Any model to calculate opacities must include bound – bound transitions as their absence can change the results by as much as a factor of two. In this paper we briefly describe the models of opacity and radiation hydrodynamics used by us and discuss some of the results on numerical simulations of hohlraum radiation temperatures. The radiation generated in the hohlraum is then used to drive the shock in a bromin doped plastic foil which has been reported in recent experiments [3]. We have also investigated the effects of different parameters like mesh size, number of frequency groups used in radiation transport and equation of state (EOS) models on the results obtained from simulations.

2. Numerical Model

Although the two dimensional codes are widely used for simulations of soft x-ray driven targets, aim of the present studies is to look into the effects of number of frequency groups and the wall mesh spacing on radiation temperature inside the hohlraum. For this we have used a simple and fast multi group, 1-D, cylindrical geometry, radiation hydrodynamic code [4] similar to MULTI [5]. The hydrodynamics is treated by solving the standard mass, momentum and energy conservation equations in one-dimensional Lagrangian geometry. The shocks are treated by Von-Neumann artificial viscous prescription. The material pressure is related to the density and internal energy through a tabulated equation of state (EOS). For a given density and internal energy, the material temperature is again obtained from tabulated EOS. Complete EOS data is generated using a three-term model [6] which separately accounts for cold electron-ion interaction, contribution due to thermal vibration of ions and thermal electronic excitations. The reliability of this EOS model has been tested by comparing the isotherms and shock Hugoniots obtained for various materials with available experimental data. As an example we show in FIG.1 the calculated Hugoniot for CHBr computed using the above model. Density, atomic number and weight of the high-density polysterene (CH)n were scaled to that of CHBr. The results agree very well with the Quotidian EOS model [7]. The laser energy deposition is calculated via inverse bremsstrahlung up to the critical density and a pre-specified fraction is dumped at the critical density to account for anomalous absorption. The thermal flux is treated using the flux limited Sptizer's formula and the radiation transport is modelled through multi group radiation diffusion or discrete direction S_n method. Tabulated opacity data is used. We use the screened hydrogenic atom model including the l splitting [8] for the calculation of the radiation opacities. The 10x10 matrix of the screening constants is used as proposed by More [9] with the additional 10 constants as given by Perrot [10]. Standard formulae are used for Lorentz and Doppler broadening while the fine structure and stark broadenings are calculated in the hydrogenic approximation. The occupation numbers P_{nl} are evaluated in an iterative manner including the effect of pressure ionization. We use a non-uniform frequency groups with a total of 5000 frequency points [11]. In FIG.2 we show the calculated opacity of the $CH_{0.946}$ $Br_{0.054}$ as a function of photon energy at temperature of 100 eV and the density of 0.4 g/cm^3. Presence of peaks at high energy indicate the usefulness of this material for preheat shield. The results are also in good agreement with the XSN model [12].

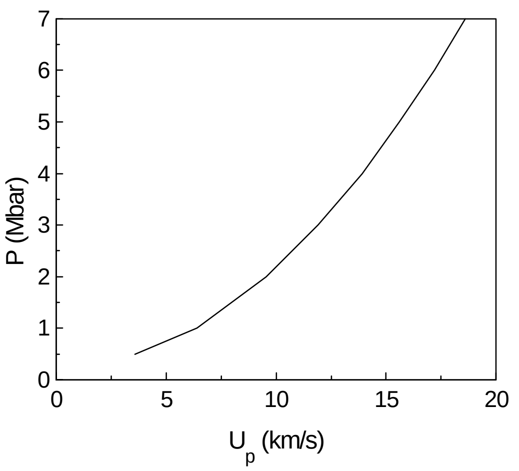

FIG. 1. Calculated ChBr Hugoniot.

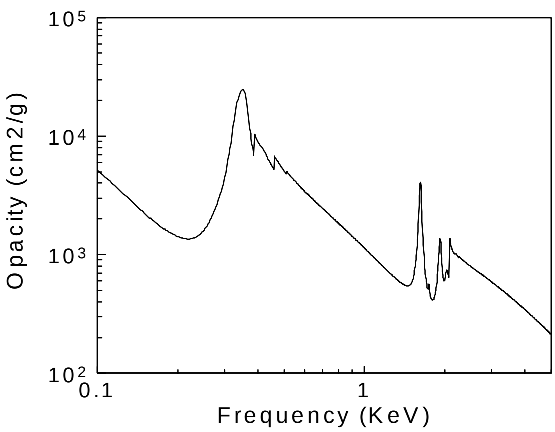

FIG. 2. Calculated Opacity for ChBr.

3. Results and Discussions

In the experiments reported using NOVA lasers, 3 mm long and 1.6 mm diameter cylindrical gold hohlraums were driven by 8 laser beams [13]. The temporally shaped 3.3 ns laser beams of wavelength 0.351 μm, each having energies from 2.0 to 3.0 kJ delivered a total peak power of 16 TW/cm^2. We have carried out numerical studies with reference to the results from this experiment using the model described earlier. EOS data tables were generated for gold using the three-term EOS model mentioned above. Rosseland and Planck means were generated in 1, 100 and 150 groups for different densities and temperatures. The multi group boundaries are taken to be equally spaced in lethargy variable. This leads to higher number of groups for lower energies. In FIG. 3 we show the time dependent radiation temperature as calculated by our code using 1, 100 and 150 groups of radiation transport. These results are for a total laser energy of 16.4 kJ incident on the inner surface of cylindrical hohlraum. The temporal shape of the incident laser beam is the same as discussed by Remington et al [13] and therefore not described here. The radiation temperature inside the cylindrical hohlraum is seen to be strongly dependent on the number of frequency groups used. A one group gray approximation is found to grossly under-predict the temperature. Comparing these results with the 2-D calculations of Remington et al [see FIG. 7 in Ref. 13] , we observe that for the case of 150 groups, foot as well as peak temperatures are well reproduced. In FIG. 4 we show the effect of mesh spacing in the hohlraum wall. In this figure, the curve marked η=1.0 refers to uniform 100 meshes. For the other two cases on mesh spacing, we used a non-uniform mesh size which increases in a geometric series with the ratio η while moving from the front (laser irradiation) side towards the inner side of hohlraum wall. This leads to fine meshes in the crucial front side region, facing laser beams. From this behaviour, it is evident that a course mesh can lead to a very strong underestimation of reemission from the walls. A uniformly sized 100 mesh simulation is not able to reproduce the peak properly in the time profile of radiation temperature and leads to a maximum temperature of only about 60 eV against the expected value of about 200 eV.

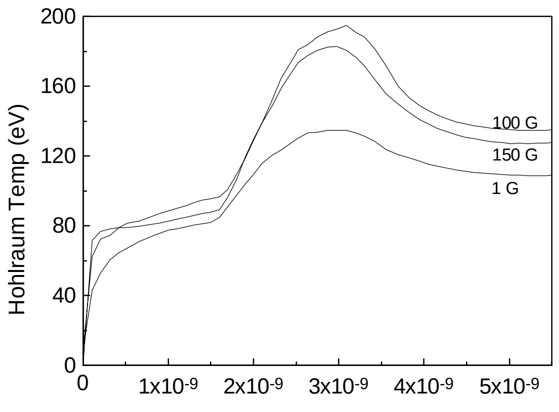

FIG. 3. Effect of Frequency Group Numbers.

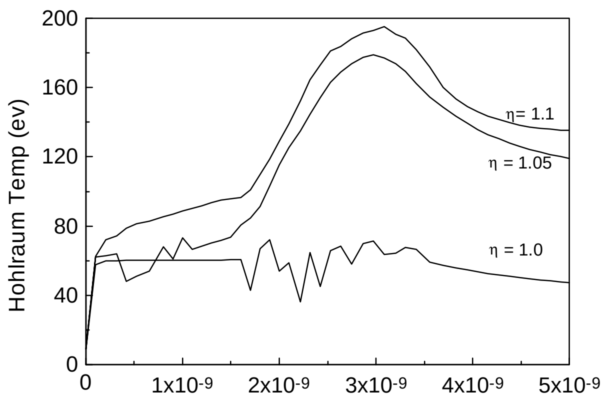

FIG. 4. Effects of Mesh Size.

In FIG.5 we show the calculated radiation spectrum inside the hohlraum. We do observe the peaks in the high energies for both, the foot (1ns) and peak (3ns). This non-Planckanian nature of spectrum suggests the possibility of preheat in the target unless care is taken in the target design to absorb such radiation.

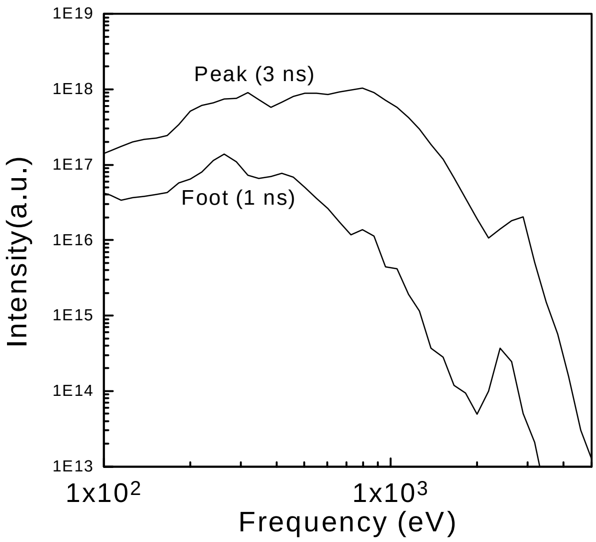

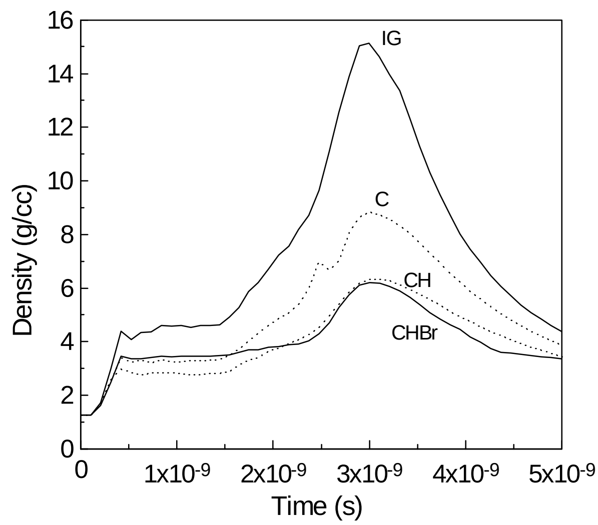

FIG. 5. Calculated Radiation Spectrum.

FIG. 6. EOS Effects on Density Profiles.

Hydrodynamics of a 0.75 mm thick $CH_{0.946}$ $Br_{0.054}$ foil driven by this hohlraum radiation was simulated using 100 groups in radiation transport. The maximum density observed at the shock front is plotted as a function of time in FIG 6 for some of the equivalent equation of state models considered by us. Comparing these results with the 1-D calculations of Remington et al. [13], we observe that the maximum compressions are well predicted by our three terms EOS model. An ideal gas EOS for the same composition of doped plastic over predicts the maximum compression by a factor of 2.5. On the other hand the use of Carbon EOS for $CH_{0.946}$ $Br_{0.054}$ leads to an over-prediction by a factor of about 1.4 which also reflects the effect of doped atoms.

Acknowledgements

We would like to express our sincere thanks to Dr. S. K. Sikka for his keen interest and discussions in this work.

References

[1] CAUBLE R. et al., Phys. Rev. Lett. **70** (1993) 2102.
[2] SANFORD R. B. et al., Phys. Rev. Lett. **83** (1999) 5511.
[3] COLOMBANT D. et al., Phys. Rev. **E 37** (1998) 3411.
[4] GUPTA N. K. and KUMAR VINOD, Laser and Particle Beams **13** (1995) 389.
[5] RAMIS R. et al., Computer Physics Communication **49** (1998) 475.
[6] GODWAL B. K. et al, Laser and Particle Beams **15** (1997) 353.
[7] GAUTHIER, J. C. et al, Laser and Particle Beams **17** (1999) 195.
[8] RICKERT A. & MEYER-TER-VEHN, J. Laser and Particle Beams **8** (1990) 715.
[9] MORE, R. M., J. Quant. Spectrosc. Radiat. Transfer **27** (1982) 345.
[10] PERROT F., Phys. Scr. **39** (1989) 332.
[11] GUPTA N. K., Report BARC/1999/E/015 (1999).
[12] WEBER S. V. et al, Phys. Plasmas **1**, (1994) 3652.
[13] REMINGTON B. A. et al, Phys. Plasmas **2**, (1995) 241.